ELSEVIER

Journal of Organometallic Chemistry 539 (1997) 131–139

Journal of Organometallic Chemistry

Stereoelectronic effects and gas phase Co^+, Ni^+, $CpFe^+$, $CpCo^+$ and $CpNi^+$ affinities of pyridines studied by the kinetic method

Philip S.H. Wong, Shuguang Ma, Feng Wang, R. Graham Cooks *

Department of Chemistry, Purdue University, West Lafayette, IN 47907-1393, USA

Received 30 October 1996; revised 8 January 1997

Abstract

Cluster ions of Co^+, Ni^+, $CpFe^+$, $CpCo^+$ and $CpNi^+$ (Cp = cyclopentadienyl) with pyridines are generated in a multi-quadrupole mass spectrometer and the kinetic method is used to examine the pyridine affinities of the cations. Absolute Co^+ and Ni^+ affinities of pyridine are both determined as 60 ± 4 kcal mol^{-1}, values which are greater than the Fe^+ affinity (49 ± 3 kcal mol^{-1}), consistent with the order of the affinities of other ligands, such as water and ammonia, to these cations. The relative metal ion and ligated-metal ion affinities of meta- and para-substituted pyridines display excellent linear correlations with the corresponding proton affinities. The slopes of the correlation lines for Co^+, Ni^+, $CpFe^+$, $CpCo^+$ and $CpNi^+$ are 0.35, 0.41, 0.52, 0.42 and 0.49 respectively, the larger slopes being for the ligated metal ions corresponding to their larger sizes and probable weaker bonding. A set of gas-phase stereoelectronic parameters S^k, measured by the deviation of the experimental data from the metal ion/proton affinity regression line, shows that steric effects due to pyridine ring substituents give rise to lower than expected affinities for the di-ortho-substituted pyridines. Steric effects also weaken the pyridine–metal bonds in the cyclopentadienyl metal ion–pyridine clusters compared to the bare metal systems. The occupancy of 4s orbitals in Fe^+ causes electronic repulsions with the pyridines and makes the steric effects larger for Fe^+ than the other metals, in spite of the fact that the Fe^+ systems are more weakly bound. © 1997 Elsevier Science S.A.

Keywords: Iron; Cobalt; Cyclopentadienyls; Pyridine; Mass spectrometry; Proton affinities

1. Introduction

The mechanism of activation of C–H or C–C bonds in hydrocarbons by transition metal ions has been studied extensively [1,2] owing to the importance of transition metal sites as active centers for the selective catalytic transformation of small molecules. Since a better understanding of these reaction mechanisms is desirable in order to improve catalysts, gas phase organometallic ion chemistry has become an increasingly active area of research during the past decade [3,4]. The gas phase is an ideal environment for the study of the intrinsic properties of metal ions; for example, by knowing metal–ligand bond dissociation energies (BDEs), one can determine whether particular mechanisms are energetically feasible.

The metal–ligand (M^+–L) BDE has been measured by a variety of methods using mass spectrometers of various types. In an ion beam apparatus [5], the cross-section for the reaction

$$M^+ + RL \rightarrow ML^+ + R$$

is measured as a function of collision energy and the metal–ligand BDE is obtained from the onset of the endothermic process. Ion cyclotron resonance [6] has been used to measure upper limits of the bond energies of transition metal ions with small organic molecules by determining the appearance threshold for the production of fragment ions. Other techniques used to measure BDEs in various types of mass spectrometer include ligand-exchange reactions and equilibrium measurements [7], kinetic energy release distributions [8], threshold collisional activation [9] and the kinetic method [10,11].

The kinetic method is based on the competitive rate

* Corresponding author.

PII S0022-328X(97)00057-0

of dissociation of a mass-selected cluster ion, e.g. $Py_1M^+Py_2$, as shown in Eq. (1):

$$Py_1M^+Py_2 \begin{cases} \xrightarrow{k_1} Py_1M^+ + Py_2 \\ \xrightarrow{k_2} Py_2M^+ + Py_1 \end{cases} \quad (1)$$

where Py_1 and Py_2 represent two different pyridines, and M^+ is the central cation. Eq. (2) expresses the relative rate constants for competitive dissociations of the cluster ion in terms of the difference in affinities of the individual monomers for the cation, M^+. It can be used to estimate the M^+ affinities of pyridines provided data are obtained for two or more reference compounds of known M^+ affinities. Alternatively, data for just one reference compound suffices, provided the effective temperature T_{eff} of the activated dimeric ion, $Py_1M^+Py_2$, is known.

$$\ln\frac{k_1}{k_2} = \ln\frac{[Py_1M^+]}{[Py_2M^+]} = \frac{\Delta(M^+\text{affinity})}{RT_{eff}} \quad (2)$$

The derivation of Eq. (2) is given in Ref. [10,11].

The kinetic method is based on the assumption of negligible or self-cancelling entropy effects and applications are usually limited to loosely-bound cluster ions which undergo simple dissociation kinetics. Such reactions usually occur with zero or very small reverse activation energies. Despite these limitations, the method has been successfully used to measure, inter alia, the proton affinities (PAs) of carboxylic acids, alcohols, amines, amino acids and phenoxy free radicals [10–14], as well as Cl^+ [15], CN^+ [16], $OCNCO^+$ [17], SF_3^+ [18], PCl_2^+ [19], $HBOCH_3^+$, $B(OCH_3)_2^+$ [20], $SiCl^+$, $SiCl_3^+$ [21] and Fe^+ [22] affinities for pyridines. Relatively little work has been on the measurements of metal ion–ligand bond dissociation energies by the kinetic method [22–32], although an early application dealt with the study of the relative silver cation affinities of alcohols [25]. The method is particularly useful for non-volatile compounds where insufficient sample vapor pressure precludes ion/molecule reaction bracketing and equilibrium measurements and it is unaffected by competing reactions such as charge transfer and proton transfer reactions which might adversely affect bracketing and equilibrium measurements.

Correlations of PAs with those for other cations have revealed the existence of gas phase stereoelectronic effects. These effects operating on the cation affinities of pyridines are well studied in a variety of chemical systems [15–22]. Ortho-substituted pyridines generally have lower cation affinities than those of their para isomers due to the steric effects of the ortho substituent(s) [15–22]. By contrast, higher than expected $SiCl^+$ affinities of ortho-substituted pyridines are observed and are ascribed to agostic effects [21]—three-center, two-electron bonding involving a central hydrogen atom—which strengthen the bond.

The goals of the present study are to determine Co^+, Ni^+, $CpFe^+$, $CpCo^+$ and $CpNi^+$ affinities of a group of alkyl-substituted pyridines and to investigate stereoelectronic effects which might arise for ortho-substituted pyridines, especially in their bonding to cyclopentadienyl (Cp)-substituted metal cations. The pyridines were chosen for study because they are strong bases in which ring substituents can be introduced to systematically modify their electronic and steric effects. The results are compared with those for Fe^+ and for other polyatomic cations examined previously [15–22].

2. Experimental

All experiments were performed using a custom-built pentaquadrupole mass spectrometer [33] comprised of three mass-analyzing quadrupoles (Q1, Q3, Q5) and two reaction quadrupoles (Q2, Q4). The ions M^+ and CpM^+ ions were generated by 70 eV electron ionization of ferrocene, cobaltocene and nickelocene. Electron ionization (EI) of these compounds generates relatively low M^+ and CpM^+ ion currents due to the low vapor pressure of these compounds and their limited fragmentation. Hence Q1 was operated in the r.f.-only mode to allow all the ions generated in the ion source to be transmitted to Q2, where they were allowed to react with a mixture of two pyridines. Particular ion/molecule reaction products formed in Q2 were mass-selected using Q3 and allowed to undergo energetic collisions with argon in Q4, while Q5 was scanned to record the product ion spectrum [34].

The bis(cyclopentadienyl) metal compounds were introduced into the ion source by evaporation from a direct insertion solids probe which was not heated. The ion source was kept at 120 °C. The indicated pressure was 5×10^{-5} Torr upon addition of a mixture of two pyridines to Q2 and increased to 7×10^{-5} Torr upon addition of the collision gas, argon, to Q4. The pressure was monitored by an ionization gauge located in the vacuum housing near Q5. The collision energy was near 0 eV in Q2 and 10 eV in Q4. All compounds are commercially available; mass/charge ratios (m/z) are reported using the Thomson unit (Th) [35].

3. Results and discussion

Fig. 1 shows the spectrum of ion/molecule reaction products formed when the ions generated by EI of cobaltocene react with a mixture of pyridine and 4-methylpyridine. The spectrum shows that there are two

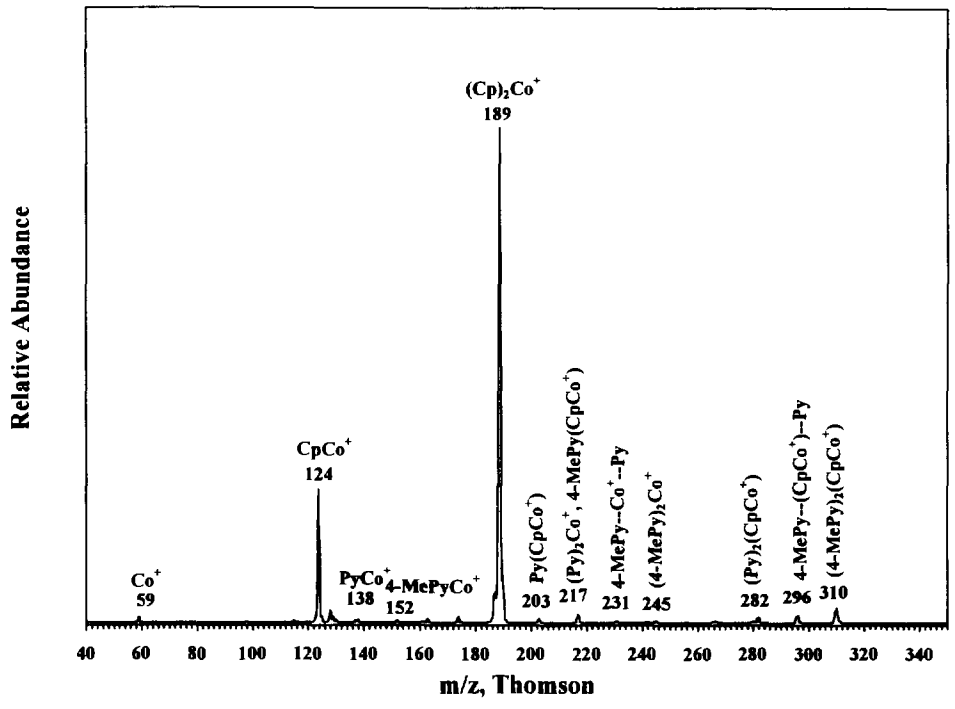

Fig. 1. Ion/molecule reaction products formed between the ions, generated by EI of cobaltocene, and a mixture of pyridine and 4-methylpyridine.

types of product, the cobalt and the cyclopentadienyl cobalt ionic clusters of the pyridines. Both the ions Co^+ and $CpCo^+$ form 1:1 (138, 152, 203 and 217 Th) and 1:2 adducts (217, 231, 245, 282, 296 and 310 Th) with the neutral pyridines. When the unsymmetrical Co^+-bound dimer of pyridine and 4-methylpyridine, 231 Th, is mass-selected in Q3 and fragmented by collision-induced dissociation (CID) with argon in the second reaction region (Q4) under mild conditions (collision energy 10 eV), the only fragments observed are the two mono-adducts, $PyCo^+$, 138 Th, and $4\text{-}MePyCo^+$, 152 Th, as shown in Fig. 2. This result, and the gentle

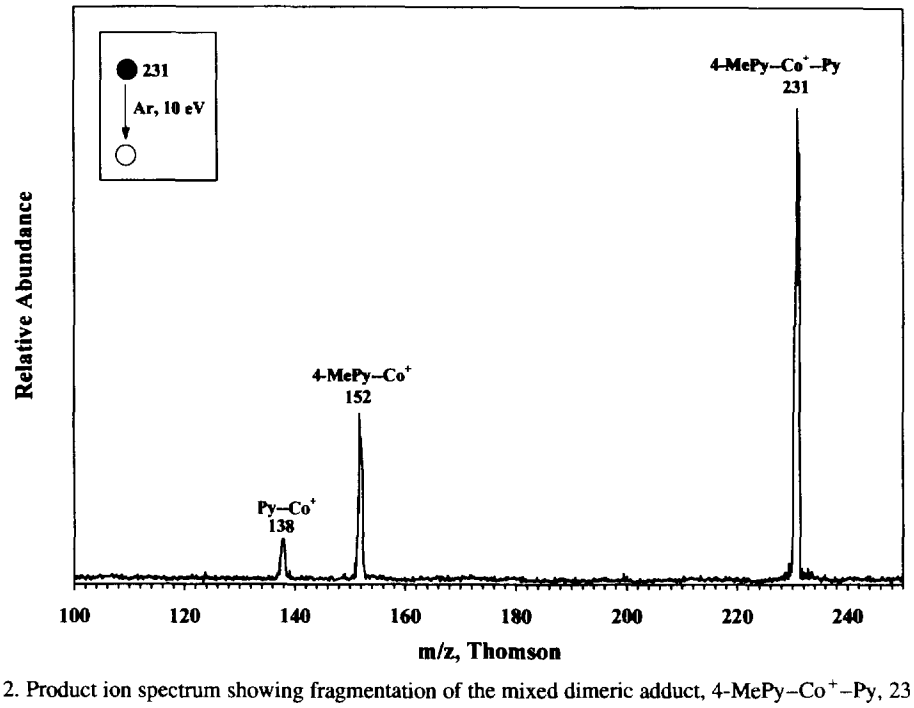

Fig. 2. Product ion spectrum showing fragmentation of the mixed dimeric adduct, 4-MePy–Co^+–Py, 231 Th.

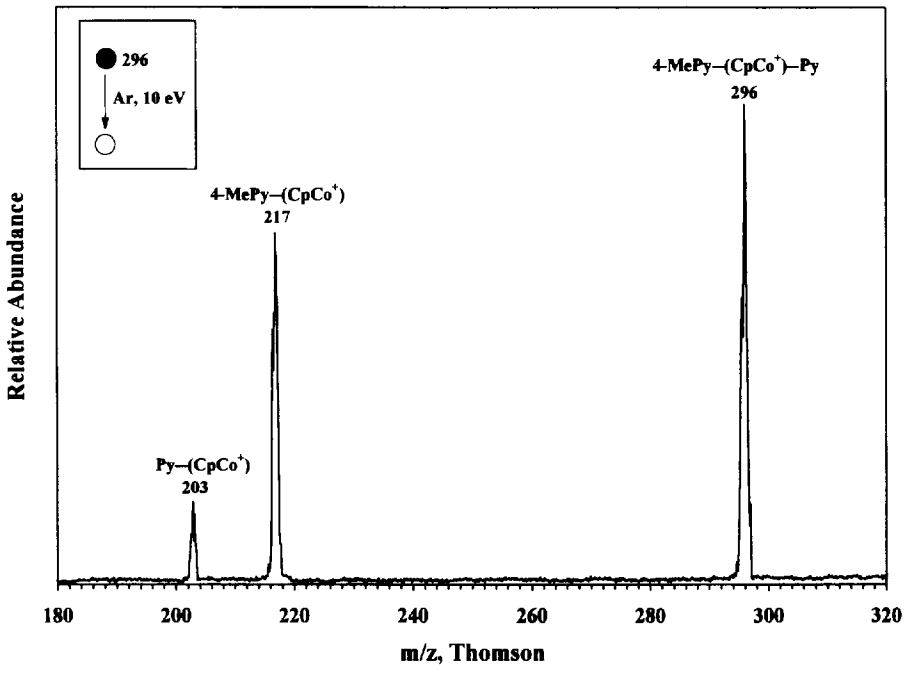

Fig. 3. Product ion spectrum showing fragmentation of the mixed dimeric adduct, 4-MePy–($CpCo^+$)–Py, 296 Th.

activation conditions under which it is obtained [15], indicates that the dimers of interest are relatively loosely bound, an observation similar to those in previous studies of other cation affinities [15–22]. Similarly, Fig. 3 shows a spectrum which displays the products of CID of the dimer 4-MePy–($CpCo^+$)–Py, 296 Th, formed from the complexed metal ion. Again, only two fragments are observed, the mono-adducts, Py($CpCo^+$), 203 Th, and 4-MePy($CpCo^+$), 217 Th. Fragmentation of the dimer 4-MePy–($CpCo^+$)–Py occurs much more readily than that of 4-MePy–Co^+–Py under the same experimental conditions and this indicates that the $CpCo^+$–Py bond is weaker than Co^+–Py bond in the dimer, presumably due to steric repulsion between the bulky cyclopentadienyl group and the pyridines. Similar results were obtained for Ni^+-, $CpNi^+$- and $CpFe^+$-bound cluster ions. The presence of a cyclopentadienyl substituent strongly affects the properties and reactivities of the metal ions. For example, $CpCo^+$ forms stronger bonds than does Co^+ (for example,

Table 1
PAs and logarithm of product ion abundance ratios for CID of cation-bound dimers of pyridines

Entry	Pyridines	Py_1:Py_2 [a]	$\ln\{[Py_1M^+]/[PyM^+]\}$ [b]						PA [c]
			Fe^+ [e]	Co^+	Ni^+	$CpFe^+$	$CpCo^+$	$CpNi^+$	
1	Py		0	0	0	0	0	0	220.4
2	3-MePy	2:1	0.9	0.95	0.95	1.48	1.20	1.37	222.8
3	4-MePy	3:1	1.3	1.26	1.61	1.82	1.52	1.83	223.7
4	4-EtPy	4:3	1.4	1.53	1.89	2.14	1.65	2.12	224.6
5	3,5-diMePy	5:3	1.8	1.83	2.12	2.72	2.19	2.58	225.5
6	3,4-diMePy	6:3	2.1	2.02	2.35	3.14	2.49	2.83	226.2
7	2-MePy	7:1	—	1.13	1.41	1.73	1.47	1.62	223.7
8	2,5-diMePy	8:3	1.7	2.01	2.28	3.19	2.52	2.88	226.2
9	2,3-diMePy	9:3	1.7	2.00	2.57	2.87	2.38	2.86	226.2
10	2,4-diMePy	10:3	2.1	2.34	2.60	3.58	2.86	3.27	226.9
11	2,6-diMePy	11:3	1.7	2.26	2.71	3.21	2.00	2.41	227.1
12	2,4,6-triMePy	12:3	2.7	3.14	3.95	4.46	3.38	3.62	230.3 [d]

[a] The entry number of the pyridine forming the cation-bound dimer used to estimate the affinities.
[b] Experimental results obtained from the average of five measurements with an average standard deviation of ±0.10.
[c] PAs are taken from Ref. [39]. This older set of values is used in preference to others because it is internally more consistent and it facilitates comparison of the present data with those for pyridine binding to other cations. See Ref. [16] for a discussion of this point.
[d] Estimated by using the combined inductive and resonance effect of 3.2 kcal mol^{-1} for a 4-methyl group and by adding this value to the PA of 2,6-dimethylpyridine (see Ref. [15]).
[e] From Ref. [22].

Table 2
Absolute and relative cation affinities of pyridines

	Absolute affinity (kcal mol^{-1})[a]			Relative affinity (kcal mol^{-1})		
	Fe^+ [b]	Co^+	Ni^+	$CpFe^+$	$CpCo^+$	$CpNi^+$
Py	49.0	60.0	60.0	0	0	0
3-MePy	50.0	60.9	60.9	1.4	1.1	1.3
4-MePy	50.4	61.2	61.5	1.7	1.5	1.8
4-EtPy	50.6	61.5	61.8	2.1	1.6	2.0
3,5-diMePy	51.0	61.8	62.0	2.6	2.1	2.5
3,4-diMePy	51.3	61.9	62.3	3.0	2.4	2.7
2-MePy	—	61.1	61.4	1.7	1.4	1.6
2,5-diMePy	50.9	61.9	62.2	3.1	2.4	2.8
2,3-diMePy	50.9	61.9	62.5	2.8	2.3	2.7
2,4-diMePy	51.3	61.2	62.5	3.4	2.7	3.1
2,6-diMePy	50.9	62.2	62.6	3.1	1.9	2.3
2,4,6-triMePy	52.0	63.0	63.8	4.3	3.2	3.5

[a] Estimated relative error ± 1 kcal mol^{-1} which is the maximum uncertainty ($\pm 15\%$) associated with the uncertainty in the effective temperature and the logarithm of the abundance ratio (e.g. 0.15×5.7 kcal mol^{-1} = 0.9 kcal mol^{-1}); estimated absolute error ± 5 kcal mol^{-1}.
[b] From Ref. [22].

BDE(Co^+–C_4H_6) < BDE($CpCo^+$–C_4H_6); BDE(Co^+–Cp) < BDE($CpCo^+$–Cp) [36]) owing to charge dispersion in $CpCo^+$. The charge transfer effect also increases the reactivity of $CpNi^+$ towards chlorobenzene by elimination of HCl while Ni^+ does not react in this way [37]. In other cases, the cyclopentadienyl group inhibits the reactivity of the metal. For example, $CpNi^+$ does not react with aromatic compounds PhX due to steric effects, where X is CH_2Br, CH_2OH, CH_2CH_3 or $(CH_2)_3CH_3$ while Ni^+ reacts to form the sets of products $C_7H_7^+ + NiBr$, $C_7H_7^+ + NiOH$, $NiPhCHCH_2^+ + H_2$, and $NiPhCH_3^+ + C_3H_6$ respectively [38]. These results show that stereoelectronic effects can either increase or decrease the reactivity. Analogous competition between gas phase steric and agostic effects was noted earlier [21]. In the current studies, the steric effect of the cyclopentadienyl group is dominant, as will be discussed in detail below.

Table 1 summarizes all the fragment ion abundance ratios obtained from the CID of the cation-bound dimers of pyridines, including, for completeness, the values for Fe^+ reported previously [22]. The Co^+ affinity of pyridine is determined by using benzene and ammonia as reference compounds. The experiment employed a mixture of pyridine and the reference compound, both introduced into quadrupole Q2. The logarithms of the fragment ion abundance ratios, ln{[Co^+–Py]/[Co^+–NH_3]} and ln{[Co^+–Py]/[Co^+–C_6H_6]}, are found to be 1.25 and -1.15 respectively upon CID of the metal ion-bound heterodimers Py–Co^+–NH_3 and Py–Co^+–C_6H_6. Hence one concludes that the Co^+ affinity of pyridine is greater than that of ammonia and smaller than that of benzene. The literature values for the Co^+–NH_3 and Co^+–benzene bond strengths are 58.8 ± 4 kcal mol^{-1} [38] and 61.1 ± 2.5 kcal mol^{-1} [40] respectively. By using Eq. (2), the Co^+ affinity of pyridine and the effective temperature are found to be 60 ± 5 kcal mol^{-1} and 484 ± 50 K respectively. The measured Co^+ affinity value is believed to be reliable because it lies in a narrow range (58.8–61.1 kcal mol^{-1}) between the bond strengths of the two reference compounds. Note that mass discrimination is insignificant in these experiments as established in earlier studies [11,41]. Note also that reference compounds are limited by the availability of suitable references with a Co^+ affinity of about 60 kcal mol^{-1}, for example H_2O cannot be used as reference compound (BDE(Co^+–H_2O) = 40.1 kcal mol^{-1}) since it will result in exclusive formation of Co^+–Py upon CID of the dimer Py–Co^+–H_2O due to the large difference in Co^+ affinities (ca. 20 kcal mol^{-1}).

The Ni^+ affinity of pyridine is determined similarly by CID of the heterodimer, Py–Ni^+–benzene, and knowing BDE(Ni^+–benzene) = 58.1 ± 2.5 kcal mol^{-1} [40]. The logarithm of the fragment ion abundance ratio, ln{[Ni^+–Py]/[Ni^+–C_6H_6]}, is found to be 1.98. Attempts to use ammonia as another reference compound were unsuccessful because the dissociation of the dimer Py–Ni^+–NH_3 resulted in the exclusive formation of $PyNi^+$ due to the much smaller Ni^+ affinity of ammonia (51.2 ± 4 kcal mol^{-1}) [38] compared to that of pyridine. Although the effective temperature of the activated Ni^+-bound dimers could not be determined independently by employing ammonia as another reference compound, the effective temperature of the Co^+-bound dimer can be assumed to be similar to that of Ni^+-bound dimers. (It has been shown that different dimer ions generated under identical conditions and having the same lifetime, also have similar effective temperatures [23,24]. This approximation has also been made in the determination of relative copper(I) affinity of amino acids where it is assumed that the effective temperature of the proton-bound dimers of amino acids is similar to that of the Cu^+-bound dimers [27].) Applying Eq. (2)

and assuming the effective temperature (484 K) measured for the Co^+-bound dimers, the Ni^+ affinity of pyridine is found to be 60 ± 4 kcal mol^{-1}. The Co^+ and Ni^+ affinities of pyridine are small in comparison (for example) with the monatomic Cl^+ affinity (201 kcal mol^{-1}) [15]; the low values are ascribed to the diffuse nature of the 3d orbitals [22] compared to the much smaller Cl^+ (ionic radius 0.86 Å [42]).

Knowing the affinity of pyridine towards the metal ions and the effective temperature of the activated clusters, the affinities of substituted pyridines can be calculated using Eq. (2) and the resulting absolute affinities are shown on Table 2. The results were cross-checked by examining the complex 4-MePy–Co^+–NH_3 which yielded a logarithm ratio, ln{Co^+–4-MePy]/[Co^+–NH_3]}, of 2.26 upon CID. This ratio yields a Co^+ affinity of 4-MePy of 61.0 kcal mol^{-1}, a value which agrees within experimental error with the value (61.2 kcal mol^{-1}) shown in Table 2. By contrast, the determination of CpM^+ affinities of pyridines via Eq. (2) is limited by the lack of suitable reference CpM^+ affinity values. However, it is still possible to compare the relative magnitudes of the CpM^+ cation affinities using the quantity ln{[$Py_1(CpM^+)$]/[$Py(CpM^+)$]}, which is directly proportional to the CpM^+ affinity difference, and the measured effective temperature of 484 K. The relative affinities so determined are also listed in Table 2. If the same electronic effects known to influence PAs also affect M^+ and CpM^+ affinities, and if these effects parallel each other, then the same order is expected for the cation affinities and PAs. Excellent linear correlations are observed between the relative M^+ and CpM^+ affinities of meta- and para-substituted pyridines and their PAs as shown in Figs. 4 and 5 in the cases of Co^+- and $CpCo^+$-bound dimers. Plots for Ni^+, $CpFe^+$and $CpNi^+$ are similar to those of Co^+ and $CpCo^+$ and so are not reproduced. The existence of the linear correlations confirms the analogies in the underlying electronic effects and also demonstrates that the dimers are symmetrically bound with respect to the central metal atom; otherwise the order of pyridine addition to the cation would affect the relative rates of dissociation. The assignment of a symmetrical structure has been confirmed by ab initio calculations in the analogous cases of Cl^+, CN^+ and $OCNCO^+$ cation-bound pyridine dimers [15–17]. The proposal that pyridines bind to the metal center by the nitrogen atom is supported by the fact that Fe^+ and Ni^+ activate the C–C and C–H bonds in the ethyl and propyl groups of 2-ethylpyridine and 2-propylpyridine respectively, resulting in the loss of H_2 and C_2H_2 [2]. The analogous reaction does not occur in 3-ethyl and 3-propylpyridine, probably because the alkyl group is too far from the metal center. Hence, the metal ion most probably binds to the nitrogen atom of the pyridines although π-binding is not excluded and there are examples of π-bonding in related systems such as benzene– and thiophene–metal complexes [43]. In the case of the pyridine/MCp^+ complexes, binding through the nitrogen atom is much more clearly established than in the simple metal complexes as the stereoelectronic parameter S^k increases dramatically between the mono-ortho-substituted pyridines and the di-ortho-substituted pyridines (see Fig. 5); the S^k values should be similar if binding were through the π-system of the pyridine.

The linear relationship between the logarithm of fragment ion abundance ratios and the corresponding PAs can be characterized by the equation ln{[Py_1M^+)]/[PyM^+)]} = m(PA) + b, where m and b are respectively the slope and the intercept of the linear regression line. Table 3 summarizes the slopes and intercepts for the cations studied. The slope is a measure of the sensitivity of the central cation to the effects of ligands. The ligated metal ions have larger slopes (0.52, 0.42 and 0.49) than the corresponding bare metal ions (0.35, 0.35 and 0.41), perhaps owing to the bond-weakening steric effect of the cyclopentadienyl group.

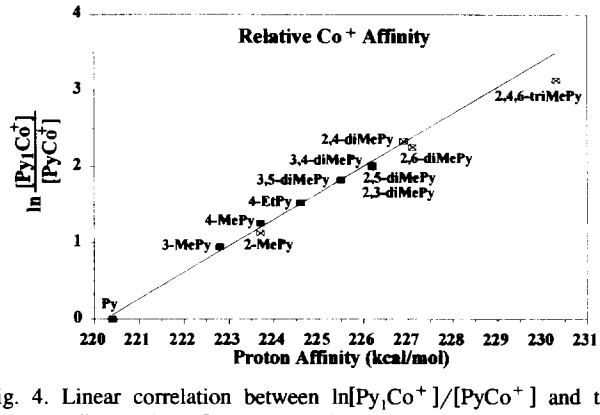

Fig. 4. Linear correlation between ln[Py_1Co^+]/[$PyCo^+$] and the corresponding PAs. Open symbols represent ortho-substituted pyridines. The correlation line is established by the points due to the meta- and para-substituted pyridines (the solid symbols).

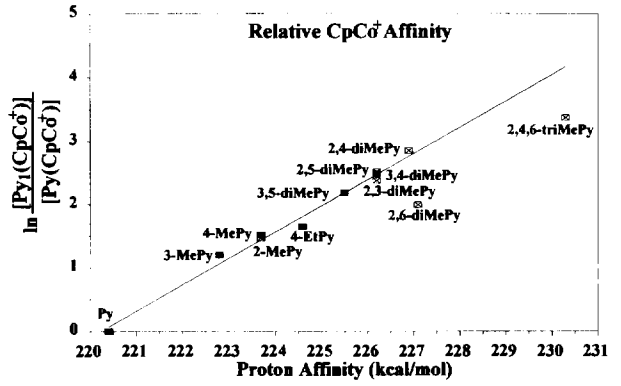

Fig. 5. Linear correlation between ln[$Py_1(CpCo^+)$]/[$Py(CpCo^+)$] and the corresponding proton affinities. Open symbols represent ortho-substituted pyridines. The correlation line is established by the points due to the meta- and para-substituted pyridines (the solid symbols).

Table 3
Parameters of the linear regressions, bond energies, ionic radii, ground state electronic configurations of the metal ions and the stereoelectronic parameter S^k

Ion	Slope	Intercept	Correlation coefficient, r^2	Bond energy, Py–M^+ (kcal mol^{-1})	Ionic radius [c] (Å)	Ground state electronic configuration	S^k [e]	
							2,6-diMePy	2,4,6-triMePy
Fe^+	0.35 [d]	−76.9 [d]	0.9915 [d]	49 ± 3 [d]	1.1	$4s3d^6(^6D)$ [a]	−0.7 [d]	−0.8 [d]
Co^+	0.35	−76.7	0.9952	60 ± 4	1.07	$3d^8(^3F)$ [a]	−0.1	−0.4
Ni^+	0.41	−91.3	0.9813	60 ± 4	1.05	$3d^9(^2D)$ [a]	−0.0	−0.2
$CpFe^+$	0.52	−115.6	0.9922	—	—	$4s^23d^{10}$ [b]	−0.4	−0.8
$CpCo^+$	0.42	−91.4	0.9853	—	—	$4s^23d^{10}4p$ [b]	−0.9	−0.8
$CpNi^+$	0.49	−107	0.9914	—	—	$4s^23d^{10}4p^2$ [b]	−0.9	−1.3

[a] From Ref. [44].
[b] Probable electronic configuration of the ligated metal ion.
[c] From Ref. [42].
[d] From Ref. [22].
[e] Estimated uncertainty ±0.1.

Entropy-driven inversions of fragment ion abundance ratios have been reported in ions of high vs. low internal energy deposited in the course of activation of cation- or proton-bound dimers [27,45]. The entropy effect can be measured by varying the internal energy deposition in the dimer ion [27]. In order to test the assumption of negligible entropy effects made in this study, the dissociation of Co^+-bound dimers of pyridines was examined at a higher collision energy (20 eV). The results showed that the entropy effect, $T(\Delta S)$, is less than 0.6 kcal mol^{-1}. This finding justifies the assumption of negligible entropy effects; this result was expected as the series of pyridines used in this study are structurally similar.

Table 2 shows that the metal–pyridine bond strengths fall in the order $Fe^+ < Co^+ \approx Ni^+$. The same order is also found for M^+–H_2O and M^+–NH_3 systems. The M^+–H_2O bond strengths are 32.8 kcal mol^{-1}, 40.1 kcal mol^{-1} and 39.7 kcal mol^{-1}, while the M^+–NH_3 bond strengths are 38.5 kcal mol^{-1}, 58.8 kcal mol^{-1} and 51.2 kcal mol^{-1} for Fe^+, Co^+ and Ni^+ [38] respectively, with an uncertainty of ±4 kcal mol^{-1}. Theoretical calculations [42] have shown that the ionic radii of ground state Fe^+, Co^+ and Ni^+ are 1.10 Å, 1.07 Å and 1.05 Å respectively. The increase in metal–ligand bond strength from Fe^+ to Ni^+ is partly due to the decrease in size of the cations. The relatively weak Fe^+–ligand bond is probably due to the occupancy of 4s orbitals in both the ground state $^6D(4s3d^6)$ and excited state $^4D(4s3d^6)$ of Fe^+ which were generated by 70 eV EI of $Fe(CO)_5$ in previous studies [22]. It has also been shown that electron ionization (50 eV) of $Fe(CO)_5$ generates about 39% and 37% of these two states of Fe^+ respectively [46]. The 4s electron has repulsive interactions [4,44] with the dative bonding electrons of the nitrogen atom of the pyridine, resulting in a weaker bond. In order to reduce repulsion, the metal ion can be promoted to an electronic configuration (4s–3d hybridization) suitable for forming a strong dative metal–ligand bond (by removing metal electron density from the bond axis) [4]. This promotion energy is paid for by the decreased metal–ligand bond strength.

It has been shown previously that the presence of an alkyl substituent at the ortho-position of a pyridine lowers the Cl^+ [15], CN^+ [16], $OCNCO^+$ [17], SF_3^+ [18], PCl_2^+ [19], $HBOCH_3^+$, $B(OCH_3)_2^+$ [20], $SiCl_3^+$ [21] and Fe^+ [22] cation affinities. Studies on the Ni^+ affinities of alkyl amines [24] have also shown that the Ni^+ affinities of the amines decrease as the α-position becomes more branched, e.g. the Ni^+ affinity of t-$C_4H_9NH_2$ (PA = 221.3 kcal mol^{-1}) < s-$C_4H_9NH_2$ (PA = 220.5 kcal mol^{-1}) < n-$C_4H_9NH_2$ (PA = 219.0 kcal mol^{-1}). This effect was attributed to steric hindrance due to the alkyl group rather than being an artifact such as a chelation effect due to the additional ortho methyl group. A measure of this effect—S^k, the gas-phase stereoelectronic parameter—is given by the deviation of the experimentally measured logarithm of the ion abundance ratio from the linear regression line established by meta- and para-substituted pyridines [15]. In the present study of bare and ligated-metal ion affinities, the ortho-alkyl-substituted pyridines show very small steric effects (Figs. 4 and 5). This result stands in contrast to other atomic ions and especially polyatomic cations. Strong steric effects, points lying well below the regression line, are found only in the cyclopentadienyl metal clusters with di-ortho-substituted pyridines. Table 3 summarizes the stereoelectronic parameters S^k for 2,6-dimethylpyridine and 2,4,6-trimethylpyridine for the bare and ligated-metal ions. Note that the uncertainty in the S^k value is about ±0.1 and most of the S^k values are much greater than 0.1 and thus are statistically significant. Larger steric effects are found for CpM^+ ions compared with the corresponding bare M^+ ions owing to the bulky cyclopentadienyl group. For example, the S^k values for

2,6-dimethylpyridine and 2,4,6-trimethylpyridine in the Ni^+-bound dimers are 0.0 and −0.2 respectively, while the corresponding S^k values for $CpNi^+$ ion-bound dimers are −0.9 and −1.3. Steric effects of the cyclopentadienyl group have been observed in the reactions of $CpNi^+$ with some aromatic compounds [37], as discussed above. The relatively large S^k values in Fe^+, compared with Co^+ and Ni^+, are probably due to the larger size of Fe^+ (see Table 3) and the repulsive interactions between the 4s electron in Fe^+ and the ortho-substituted methyl group(s). The small S^k values in $CpFe^+$ relative to $CpCo^+$ and $CpNi^+$ may be due to the fact that $CpFe^+$ is a 12-electron complex which fully utilizes the 4s and 3d orbitals for bonding while $CpCo^+$ and $CpNi^+$, 13- and 14-electron complexes respectively, involve the occupancy of the 4p orbitals. The extra one and two non-bonding electrons, in $CpCo^+$ and $CpNi^+$ respectively, might cause relatively stronger electron–electron repulsion with the ortho-substituted pyridines, resulting in the steric effect which falls in the order $CpFe^+ < CpCo^+ < CpNi^+$ as shown by the S^k values in Table 3. The S^k values for the bare metal ions are much smaller than those of the polyatomic ions studied previously, for example, the S^k values for 2-methylpyridine in the $OCNCO^+$- and SF_3^+-bound dimers are −1.39 [17] and −1.09 [18] respectively. This is due to the smaller size of the monatomic metal ions and the weaker metal–ligand bond strength.

4. Conclusions

The kinetic method has been applied to determine Co^+, Ni^+, $CpFe^+$, $CpCo^+$ and $CpNi^+$ affinities of pyridines. Remarkably, the M^+ and CpM^+–pyridine bond energies parallel those of the corresponding pyridine–proton bond energies as is evident from the excellent linear correlations between the logarithm of the fragment ion abundance ratios and the PAs of the meta- and para-substituted pyridines. Steric effects decrease the affinities found for ortho-substituted pyridines, but these effects are much smaller than those of the polyatomic cations and can only be observed in 2,6-dimethylpyridine and 2,4,6-trimethylpyridine, the di-ortho-substituted compounds. The cyclopentadienyl group exerts a strong steric effect and weakens the CpM^+–pyridine bond compared to that of the bare metal. The information provided by the kinetic method on metal–pyridine bond strengths and stereoelectronic effects in metal ion/pyridine clusters is representative of the type of information that should be available for other systems.

Acknowledgements

This work was supported by the National Science Foundation, CHE 92-23791.

References

[1] (a) H. Schwarz, Acc. Chem. Res. 22 (1989) 282. (b) D.A. Peake, M.L. Gross, D.P. Ridge, J. Am. Chem. Soc. 106 (1984) 4998.
[2] P.S.H. Wong, S. Ma, R.G. Cooks, Rapid Commun. Mass Spectrom. 10 (1996) 927.
[3] (a) P.B. Armentrout, S.K. Loh, K.M. Ervin, J. Am. Chem. Soc. 106 (1984) 1161. (b) J. Allison, B. Radecki, J. Am. Chem. Soc. 106 (1984) 946. (c) K.R. Lane, L. Sallans, R.R. Squires, Organometallics 4 (1985) 408. (d) K. Eller, H. Schwarz, Chem. Rev. 91 (1991) 1121. (e) B.S. Freiser, J. Mass Spectrom. 31 (1996) 703.
[4] B.S. Freiser (Ed.), Organometallic Ion Chemistry, Kluwer, Dordrecht, 1996.
[5] (a) R. Houriet, L.F. Halle, J.L. Beauchamp, Organometallics 2 (1983) 1818. (b) J.L. Elkind, P.B. Armentrout, J. Chem. Phys. 84 (1986) 4862.
[6] R.L. Hettich, T.C. Jackson, E.M. Stanko, B.S. Freiser, J. Am. Chem. Soc. 108 (1986) 5086.
[7] K. Uppal, C.B. Lebrilla, T. Drewello, H. Schwarz, J. Am. Chem. Soc. 110 (1988) 3069.
[8] P.A.M. Van Koppen, D.B. Jocobson, A. Illies, M.T. Bowers, M. Hanratty, J.L. Beauchamp, J. Am. Chem. Soc. 111 (1989) 1991.
[9] (a) R.H. Schultz, P.B. Armentrout, J. Am. Chem. Soc. 113 (1991) 729. (b) J.A. Paulino, R.R. Squires, J. Am. Chem. Soc. 113 (1991) 5573.
[10] (a) R.G. Cooks, T.L. Kruger, J. Am. Chem. Soc. 99 (1977) 1279. (b) S.A. Mcluckey, D. Cameron, R.G. Cooks, J. Am. Chem. Soc. 103 (1981) 1313.
[11] R.G. Cooks, J.S. Patrick, T. Kotiaho, S.A. McLuckey, Mass Spectrom. Rev. 13 (1994) 287.
[12] (a) L.G. Wright, S.A. McLuckey, R.G. Cooks, K.V. Wood, Int. J. Mass Spectrom. Ion Processes 42 (1982) 115. (b) G. Boand, R. Houriet, T.J. Gaumann, J. Am. Chem. Soc. 105 (1983) 2203. (c) J.S. Brodbelt, R.G. Cooks, Talanta 36 (1989) 255.
[13] (a) T.K. Majumdar, F. Clairet, J.-C. Tabet, R.G. Cooks, J. Am. Chem. Soc. 114 (1992) 2897. (b) Z. Wu, C. Fenselau, Rapid Commun. Mass Spectrom. 6 (1992) 403. (c) G. Bojesen, J. Am. Chem. Soc. 109 (1987) 5557.
[14] (a) S.H. Hoke II, S.S. Yang, R.G. Cooks, D.A. Hrovat, W.T. Borden, J. Am. Chem. Soc. 116 (1994) 4888. (b) G. Chen, N. Kasthurikrishnan, R.G. Cooks, Int. J. Mass Spectrom. Ion Processes 151 (1995) 69.
[15] M.N. Eberlin, T. Kotiaho, B.J. Shay, S.S. Yang, R.G. Cooks, J. Am. Chem. Soc. 116 (1994) 2457.
[16] S.S. Yang, O. Bortolini, A. Steinmetz, R.G.Cooks, J. Mass Spectrom. 30 (1995) 184.
[17] S.S. Yang, G. Chen, S. Ma, R.G. Cooks, F.C. Gozzo, M.N. Eberlin, J. Mass Spectrom. 30 (1995) 807.
[18] P.S.H. Wong, S. Ma, S.S. Yang, R.G. Cooks, F.C. Gozzo, M.N. Eberlin, J. Am. Soc. Mass Spectrom. 8 (1997) 68.
[19] S. Ma, P. Wong, R.G. Cooks, Int. J. Mass Spectrom. Ion Processes, in press.
[20] S. Ma, P. Wong, R.G. Cooks, J. Mass Spectrom. 32 (1997) 159.
[21] S.S. Yang, P. Wong, S. Ma, R.G. Cooks, J. Am. Soc. Mass Spectrom. 7 (1996) 198.
[22] S. Ma, P. Wong, S.S. Yang, R.G. Cooks, J. Am. Chem. Soc. 118 (1996) 6010.
[23] L.Z. Chen, J.M. Miller, Org. Mass Spectrom. 27 (1992) 883.
[24] L.Z. Chen, J.M. Miller, J. Organomet. Chem. 448 (1993) 225.
[25] S.A. McLuckey, A.E. Schoen, R.G. Cooks, J. Am. Chem. Soc. 104 (1982) 848.
[26] F. Strobel, D.P. Ridge, Inorg. Chem. 27 (1988) 891.
[27] B.A. Cerda, C. Wesdemiotis, J. Am. Chem. Soc. 117 (1995) 9734.
[28] (a) C.C. Liou, J.S. Brodbelt, J. Am. Soc. Mass Spectrom. 3

(1992) 543. (b) C.C. Liou, J.S. Brodbelt, J. Am. Chem. Soc. 114 (1992) 6761.
[29] D.H. Russell, E.S. McGlohon, L.M. Mallis, Anal. Chem. 60 (1988) 1818.
[30] (a) L. Operti, G.A. Vaglio, J.R. Gord, B.S. Freiser, Organometallics 10 (1991) 104. (b) L. Operti, E.C. Tews, B.S. Freiser, J. Am. Chem. Soc. 110 (1988) 3847.
[31] I.H. Chu, H. Zhang, D.V. Dearden, J. Am. Chem. Soc. 115 (1993) 5736.
[32] K. Eller, H. Schwarz, Organometallics 8 (1989) 1820.
[33] J.C. Schwartz, K.L Schey, R.G. Cooks, Int. J. Mass Spectrom. Ion Processes 101 (1990) 1.
[34] (a) J.C. Schwartz, A.P. Wade, C.G. Enke, R.G. Cooks, Anal. Chem. 62 (1990) 1809. (b) R.G. Cooks, J. Amy, M. Bier, J.C. Schwartz, K.L. Schey, Adv. Mass Spectrom. 11A (1989) 33. (c) V.F. Juliano, F.C. Gozzo, M.N. Eberlin, C. Kascheres, C.L. Lago, Anal. Chem. 68 (1996) 1328.
[35] R.G. Cooks, A.L. Rockwood, Rapid Commun. Mass Spectrom. 5 (1991) 93.
[36] D.B. Jacobson, B.S. Freiser, J. Am. Chem. Soc. 107 (1985) 7399.
[37] R. Stepnowski, J. Allison, J. Am. Chem. Soc. 111 (1989) 449.
[38] P.J. Marinelli, R.R. Squires, J. Am. Chem. Soc. 111 (1989) 4101.
[39] D.H. Aue, M.T. Bowers, in: M.T. Bowers (Ed.), Gas Phase Ion Chemistry, vol. 2, Academic Press, New York, 1979.
[40] F. Meyer, F.A. Khan, P.B. Armentrout, J. Am. Chem. Soc. 117 (1995) 9740.
[41] L.G. Wright, S.A. McLuckey, R.G. Cooks, K.V. Wood, Int. J. Mass Spectrom. Ion Phys. 42 (1982) 115.
[42] T.K. Ghanty, S.K. Ghosh, J. Phys. Chem. 98 (1994) 9197.
[43] R. Bakhtiar, D.B. Jacobson, J. Am. Soc. Mass Spectrom. 7 (1996) 938.
[44] P.B. Armentrout, Annu. Rev. Phys. Chem. 41 (1990) 313.
[45] H.-F. Grützmacher, A. Caltapanides, J. Am. Chem. Soc. Mass Spectrom. 5 (1994) 826.
[46] P.R. Kemper, M.T. Bowers, J. Phys. Chem. 95 (1991) 5134.